Proceedings World Geothermal Congress 2020+1
Reykjavik, Iceland, April - October 2021

Exergoeconomic, exergy and energy analysis of a geothermal two-stage absorption refrigeration system

Wang Yongzhen[12], Yin Hongmei[2], Zhao Wei[1], Zhang Jing [1] DuYanping[3], ZhaoJun[2], Luo Xianglong[4], Gong Yulie[5]

1.Dept. of Electrical Engineering, Energy Internet Research Institute, Tsinghua University, Beijng, 100084, China;

2.Key Laboratory of Efficient Utilization of Low and Medium Grade Energy (Tianjin University), Tianjin, 300350, China;

3.China-UK Low Carbon College, Shanghai Jiao Tong University, Shanghai, 200240, China;

4.Faculty of Material and Energy Guangdong University of Technology, Guangzhou, 510006, China;

5.Guangzhou Institute of Energy Conversion, Chinese Academy of Science, Guangzhou, 510640, China;

E-mail address:wyz80hou@mail.tsinghua.edu.cn

Keywords: Geothermal energy; absorption refrigeration system; geothermal power plant; exergoeconomic analysis

ABSTRACT

How to realize the maximum utilization of geothermal energy becomes a key issue in the sustainable development and utilization of geothermal energy. With a concern about the waste of vast geothermal water during the operation of flash geothermal power plant in China, this paper proposes cascading a two-stage LiBr-H2O absorption refrigeration system (TSARS) to the original flash power generation system, so as to improve the utilization efficiency of the geothermal water. And, the exergoeconomic, exergy and energy model of TSARS is established to analyze the thermodynamic and economic performance of geothermal TSARS. Namely, modes of the waste geothermal water cascaded to TSARS are compared, including series and parallel modes. It is found that, although parallel TSARS is not good as series TSARS in the view of energy and exergy efficiencies, the parallel TSARS is better than the series one in the view of the exergoeconomic performance. For instance, when the geothermal water cost is about 0.211$/GJ, the chilled water exergoeconomic cost of series TSARS is about 1.06 times that of the parallel one. In addition, the exergoeconomic analysis of each equipment for parallel TSARS is made to explore the more optimal potential.

1. INTRODUCTION

Geothermal energy is derived from the heat released during fission of materials within the earth. The fission energy, so huge and long-lasting within the earth, can reach the earth crust through thermal radiation, heat convection and heat conduction [1]. The reserve of geothermal energy is not as rich as solar energy and wind energy, but the reserve is still considerable and widely distributed as a native energy. Meanwhile, the geothermal energy is stable with high utilization coefficient compared with solar energy, wind energy, biomass and other renewable sources [2]. Nowadays, scholars pay more and more attention to the utilization of geothermal energy all over the world. Geothermal power generation has been realized in 27 countries around the world by 2015 according to the statistics of World Geothermal Conference. The installed geothermal power generation capacity has exceeded 12 GW. Wherein, geothermal energy, which is mainly distributed with medium and low temperature in China, has been widely used for heating, bathing, heat pumps, power generation etc.[3,4]. However, the existing geothermal energy power plants only include Yangbajing, Yangyi and Fengshun Geothermal Power Plants, with a total capacity about 50MW. In Fengshun Flash Geothermal Power Plant, geothermal water of 91 ℃ is pumped into a flash evaporator for flashing geothermal steam, thereby driving the geothermal steam turbine to generate power. However, investigations show that a great amount of un-flashed geothermal water is not further utilized, and it is abandoned directly with the temperature range from 68 ℃ from 75 ℃ [5]. Obviously, the geothermal water is utilized in a smaller temperature difference and the relatively lower utilization rate of the geothermal water.

In fact, the utilization rate of geothermal fluid can be improved effectively by the geothermal comprehensive utilization system combining power generation and direct utilization, so as to improve the thermodynamic performance of the geothermal utilization system in accordance with the principles of energy cascade comprehensive utilization [6,7]. Namely, geothermal comprehensive utilization system can be realized by coupling and integrating geothermal power generation, refrigeration, heat supply, hydrogen production, carbon capture and other technologies [8-13]. For example, T.A.H. Ratlamwala et al. [14] realized a geothermal comprehensive utilization by feeding geothermal water through a two-stage flash power generation cycle, a four-effect ammonia absorption refrigeration cycle, a waste water heat exchange cycle and a hydrogen production cycle in series; The influence of geothermal water temperature, pressure and environment temperature on the system performance was modeled and analyzed. Oguz Arslan et al. [15] performed a comprehensive utilization of a geothermal resource in Turkey, which was used successively for organic Rankine cycle power generation, residential heating, greenhouse aquaculture and hot spring bathing. Duccio Tempesti et al. [16] studied a solar-geothermal coupling organic Rankine cycle power generation system, and the efficiency of system power generation in different months was analyzed. Can Coskun et al. [17] analyzed the form of different geothermal comprehensive utilization systems in different seasons thermodynamically. Mehmet Kanoglu, et al. [18] completed thermodynamic and economic evaluation on three possible combination systems of geothermal power generation, refrigeration and heating respectively.

Therefore, inspired by geothermal comprehensive utilization, some investigators observed the advantages of a two-stage LiBr-H2O absorption refrigeration system (TSARS) on the recovery of low-grade thermal energy, to improve the performance of geothermal utilization in Fengshun Flash Power Plant of China according to the local hot summer and warm winter climate [5, 19]. Specifically, the un-flashed geothermal waste water from the geothermal flash power plant was cascaded to TSARS, to form a geothermal cascade comprehensive utilization system for power and cooling. Hence, the utilization rate of geothermal water increased on the one hand, and the cooling capacity was generated to meet the refrigeration demand on the other hand. However,

TSARS is complex with high investment, and its coefficient of performance (COP) is lower than that of traditional electric refrigeration. Therefore, there is a trade-off between thermodynamic gain and economic investment. Then, exergy analysis method has been applied in absorption refrigeration system analysis to explore the improvement of thermodynamic performance of the system in recent years. For example, Sencan et al. [20] studied the influence of generator temperature, condensation temperature, evaporation temperature on COP and exergy efficiency of absorption refrigeration cycle. However, the economic performance of the system was not considered in the exergy analysis method. In fact, the comprehensive performance in thermodynamics and economics of the system can be analyzed and evaluated by the exergoeconomic method. For example, R.D. Misra, et al. [21,22] studied the performance of the double effect absorption refrigeration cycle and the ammonia absorption refrigeration cycle respectively according to the exergoeconomic method.

In summary, it is proposed in the paper that TSARS is applied to the recovery of the geothermal waste water in the geothermal flash power plant, and a geothermal combined power and cooling cascade comprehensive utilization system is established. Firstly, the operating data of the power plant is regarded as the benchmark for obtaining the exergoeconomic cost of geothermal water. Secondly, the exergoeconomic, exergy and energy analysis methods are utilized for studying and comparing the performance advantages and disadvantages of two modes (series and parallel) for cascading waste geothermal water to TSARS. Finally, the influences of geothermal water inlet temperature on TSARS exergoeconomic performance are analyzed. In addition, a specific case model is designed to study the exergoeconomic performance of TSARS driven by geothermal water.

2. OPERATING CONDITIONS OF GEOTHERMAL FLASH POWER PLANT IN CHINA

A single-stage flash power generation cycle is adopted in Fengshun Geothermal Power Plant in China. The flow chart of the power plant is shown in Figure 1. The geothermal water with 91℃ out of the production wells (PW) is transported to a flash evaporator (FE) through a production well pump (P). The geothermal water in the flash evaporator is flashed to generate steam by controlling the flash pressure (Pf.). The geothermal steam is fed into the steam turbine (ST) for driving the power generator (G) to generate power. Waste steam after acting through the steam turbine is fed into condenser (CON-P), which is directly cooled by cooling water (CW). It is discovered in the survey that the remaining un-flashed geothermal water in the flash evaporator is directly discharged at a flow capacity of 60 kg/s and a maximum temperature of 75 ℃. Therefore, the geothermal water utilization rate of the flash power plant is only 24.3% when environment temperature is 25 ℃.

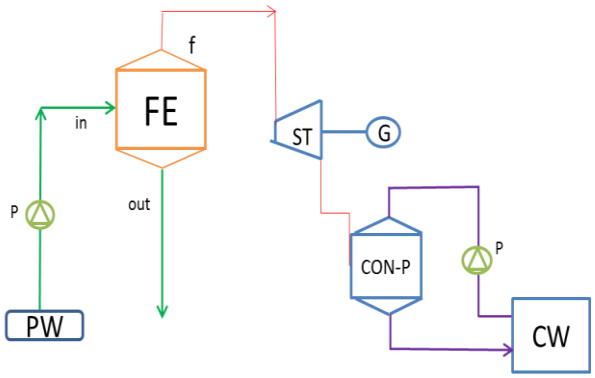

PW indicates production well; FE, flash evaporator; P, production well pump; ST, steam turbine; G, power generator; CON-P, condenser of plant; CW, cooling water

Figure 1: Flow chart of geothermal power plant in Fengshun, China

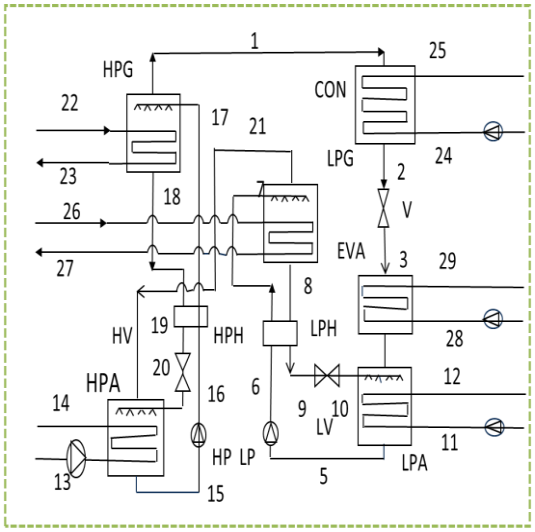

EVP indicates evaparator; LPA, low pressure abosorber; LPG, low pressure generator; LPH, low pressure heat exchhanger; HPA, high pressure absorber; HPG, high pressure generator; HPH, high pressure heat exchanger; CON, condenser; LP, low pressure solution pump; HP, high pressure solution pump; LV, low pressure valve; HV, high pressure valve;

Figure 2: Cycle flow chart of TSARS

3. ABSORPTION REFRIGERATION CYCLE OF GEOTHERMAL WASTE WATER

As above-mentioned, the thermodynamic characteristics of waste geothermal water in the geothermal power plant is considered for the newly added cooling subsystem for the geothermal waste water discharged from the power plant after geothermal flash power generation is cascaded to TSARS. A geothermal cascade comprehensive utilization system with power and cooling is formed, to improve the utilization rate of geothermal water. The absorption refrigeration technology has a greater potential in the aspects of low-grade energy utilization and industrial waste heat recovery. So, TSARS has the fewer requirements for heat source temperature than the single effect absorption refrigeration system [5,19]. Hot water higher than 60 ℃ can be applied for driving TSARS, and the above-mentioned geothermal waste water can be further utilized accordingly. The cycle flow chart of TSARS is shown in Figure 2, and more details can be found in Reference 19. In fact, there are two possible modes (series and parallel supply) for cascading geothermal waste water to TSARS, as shown in Figure 3.

a: Series mode b. Parallel mode

Figure 3. The possible ways for geothermal waste water entering into TSARS (a: Series mode, b: Parallel mode)

4. EXERGOECONOMIC ANALYSIS MODEL OF REFRIGERATION SYSTEM

The energy production system is divided into several subsystems and several exergy flows according to exergoeconomics, and then the relationship between each exergy flow and the subsystem is described, so as to obtain the exergy cost equilibrium equation and complementary equation of each subsystem; the unit exergoeconomic cost of each subsystem can be known [22, 23]. The exergy cost is defined as the exergy amount required for a material flow in unit time, and it is expressed in E, kW/s. The exergoeconomic cost is defined as the cash value consumed by a material flow within unit time, and it is expressed in C, $/s. The unit exergoeconomic cost represents the cash value required by the production unit exergy flow, expressed in c, $/J. The relationship among C, c and E is shown as follows:

$$\dot{C} = c * \dot{E} = c * \dot{m} * e \quad (1)$$

$$e = (h - h_0) - T_0 * (s - s_0) \quad (2)$$

$$\dot{E}_D = \dot{E}_F - \dot{E}_P - \dot{E}_L \quad (3)$$

Wherein, e refers to unit mass exergy, kW/kg; h is unit mass enthalpy, kJ/kg; s is to unit mass entropy, kJ/(kg•K); ED, EL, EF and EP represent system internal exergy loss, external exergy loss, input fuel exergy and output product exergy respectively.

The refrigeration system calculation model is established under the precondition of the following assumptions: 1) The system is steadily operated, and all heat exchangers undergo heat insulation treatment; 2) Refrigerant is saturated in the condenser inlet and evaporator outlet; 3) Pressure loss in pipeline and heat exchanger pressure loss due to friction is not considered; 4) The kinetic energy and chemical energy of lithium bromide solution are not considered; 5) The lithium bromide aqueous solution in the system is balanced; 6) Geothermal fluid is regard as water in the view of thermodynamic properties; 7) The temperature of lithium bromide concentrated solution in the high and low pressure throttle vales should be higher than the crystallization temperature under the pressure by 8 ℃ at least in order to prevent the lithium bromide solution from crystallizing.

4.1. Subsystem division of TSARS

There is a subsystem in each thermodynamic process of equipment in TSARS. “Fuel - Product - Loss” of each subsystem of TSARS is defined in Table 1. Therefore, input cost is equal to output cost according to the exergoeconomic balance equation.

$$\sum \dot{C}_{in,k} + \dot{Z}_k = \sum \dot{C}_{out.k} \quad (4)$$

Wherein, ($/s) denotes the annualized investment of each subsystem, and annualized investment refers to the relationship between equipment investment Zk and annualized coefficient o. It is worked out according to the following formula.

$$\dot{Z}_k = Z_k * o \quad (5)$$

Table 1: Definition of "Fuel - Product - Loss" of each subsystem

Subsystem	Fuel	Product	Loss
HPG	$\dot{E}_{22}-\dot{E}_{23}$	$\dot{E}_{1}-\dot{E}_{17}+\dot{E}$	0
HPA	$\dot{E}_{20}+\dot{E}_{21}$	$\dot{E}_{15}$	$\dot{E}_{14}-\dot{E}_{13}$
HPH	$\dot{E}_{18}-\dot{E}_{19}$	$\dot{E}_{17}-\dot{E}_{16}$	0
HP	$\dot{E}_{31}$	$\dot{E}_{16}-\dot{E}_{15}$	0
HV	$\dot{E}_{19}$	$\dot{E}_{20}$	0
LPG	$\dot{E}_{26}-\dot{E}_{27}$	$\dot{E}_{21}-\dot{E}_{7}+\dot{E}$	0
LPA	$\dot{E}_{10}+\dot{E}_{4}$	$\dot{E}_{5}$	$\dot{E}_{12}-\dot{E}_{11}$
LPH	$\dot{E}_{8}-\dot{E}_{9}$	$\dot{E}_{7}-\dot{E}_{6}$	0
LP	$\dot{E}_{30}$	$\dot{E}_{6}-\dot{E}_{5}$	0
LV	$\dot{E}_{9}$	$\dot{E}_{10}$	0
CON	$\dot{E}_{1}$	$\dot{E}_{2}$	$\dot{E}_{25}-\dot{E}_{24}$
V	$\dot{E}_{2}$	$\dot{E}_{2}$	0
EVA	$\dot{E}_{3}-\dot{E}_{4}$	$\dot{E}_{29}-\dot{E}_{28}$	0
cycle	$\dot{E}_{22}-\dot{E}_{23}+\dot{E}_{30}+\dot{E}_{31}+\dot{E}_{26}-\dot{E}_{27}$	$\dot{E}_{29}-\dot{E}_{28}$	$\dot{E}_{14}-\dot{E}_{13}+\dot{E}_{12}-\dot{E}_{11}+\dot{E}_{25}-$

Wherein, capital annualized coefficient [24]

$$o=\frac{\mathrm{m}(1+\mathrm{m})^{\mathrm{n}}}{(1+m)^{n}-1}*\frac{1}{n*t*3600} \quad (6)$$

In the above formula, m represents annual interest rate; n is system service life, year; and t is annual operation hours of the system, hour.

4.2 Exergoeconomic equations of TSARS

Exergoeconomic equations of each subsystem are established in Table 2.

The investment in TSARS includes investment in heat exchangers and pumps. Wherein, investment of high/low pressure generators, high/low pressure absorbers, high/low pressure solution exchangers, condenser and evaporator are figured out according to Formula （7）. The investment of pumps is got according to Formula（8）[24,25].

$$Z_{\mathrm{i}}=\mathrm{f}_{i}*(\frac{A_{i}}{A_{r}})^{0.6} \quad (7)$$

$$Z_{\mathrm{j}}=\mathrm{f}_{j}*(\frac{W_{i}}{W_{r}})^{0.5} \quad (8)$$

Wherein, heat exchange area of the heat exchanger and power consumption of the pumps are respectively determined according to the following Formulas（9） and （10）.

$$A_{i}=\frac{Q_{i}}{LMTD_{i}*K_{i}} \quad (9)$$

$$W_{i}=\frac{\dot{m}_{i}*g*H_{i}}{1000*\beta_{i}} \quad (10)$$

Wherein, Qi denotes the heat exchange capacity of the heat exchanger, kW; LMTDi is the logarithmic heat exchange temperature difference of the heat exchanger, ℃; Ki is the average heat exchange coefficient of the heat exchanger, kW/㎡; g is gravitational acceleration, m/s2; Hi is the head of the pump, m; βi is the efficiency of the pump, fi, fj, Ar and Wr are corrected parameters, which can be found in Reference 15.

Table 2. Exergoeconomic equations of each subsystem

Subsystems	Basic equations	Complementary equations
HPG	$\dot{C}_{22}-\dot{C}_{23}+\dot{Z}_{HPG}=\dot{C}_{1}-\dot{C}_{17}+\dot{C}_{18}$	$\frac{\dot{m}_1(c_1e_1-c_{17}e_{17})}{\dot{m}_1(e_1-e_{17})}=\frac{\dot{m}_{18}(c_{18}e_{18}-c_{17}e_{17})}{\dot{m}_{18}(e_{18}-e_{17})}$ $c_{22}=c_{23}$
HPA	$\dot{C}_{20}+\dot{C}_{21}-\dot{C}_{15}+\dot{Z}_{HPA}=\dot{C}_{14}-\dot{C}_{13}$	$\frac{\dot{m}_{21}(c_{21}e_{21}+c_{20}e_{20})}{\dot{m}_{21}(e_{21}+e_{20})}=\frac{\dot{m}_{15}c_{15}e_{15}}{\dot{m}_{15}e_{15}}$ $c_{13}=c_{14}$
HPH	$\dot{C}_{18}-\dot{C}_{19}+\dot{Z}_{HEX}=\dot{C}_{17}-\dot{C}_{16}$	$c_{18}=c_{19}$
HP	$\dot{Z}_{HP}+\dot{C}_{HPE}=\dot{C}_{16}-\dot{C}_{15}$	/
HV	$\dot{Z}_{HP}=\dot{C}_{16}-\dot{C}_{15}$	/
LPG	$\dot{C}_{26}-\dot{C}_{27}+\dot{Z}_{LPG}=\dot{C}_{21}-\dot{C}_{7}+\dot{C}_{8}$	$\frac{\dot{m}_{21}(c_{21}e_{21}-c_{7}e_{7})}{\dot{m}_{21}(e_{21}-e_{7})}=\frac{\dot{m}_{8}(c_{8}e_{8}-c_{7}e_{7})}{\dot{m}_{8}(e_{8}-e_{7})}$ $c_{26}=c_{27}$
LPA	$\dot{C}_{10}+\dot{C}_{4}-\dot{C}_{5}+\dot{Z}_{LPA}=\dot{C}_{12}-\dot{C}_{11}$	$\frac{\dot{m}_4(c_4e_4+c_{10}e_{10})}{\dot{m}_4(e_4+e_{10})}=\frac{\dot{m}_5c_5e_5}{\dot{m}_5e_5}$ $c_{12}=c_{11}$
LPH	$\dot{C}_{8}-\dot{C}_{9}+\dot{Z}_{LEX}=\dot{C}_{7}-\dot{C}_{6}$	$c_8=c_9$
LP	$\dot{Z}_{LP}=\dot{C}_{6}-\dot{C}_{5}$	/
LV	$\dot{Z}_{LW}=\dot{C}_{10}-\dot{C}_{9}$	/
CON	$\dot{C}_{1}-\dot{C}_{2}+\dot{Z}_{CON}=\dot{C}_{25}-\dot{C}_{24}$	$c_{24}=c_{25}\quad c_1=c_2$
V	$\dot{Z}_{V}=\dot{C}_{3}-\dot{C}_{4}$	/
EVA	$\dot{C}_{3}-\dot{C}_{4}+\dot{Z}_{EVA}=\dot{C}_{29}-\dot{C}_{28}$	$c_3=c_4\quad c_{28}=c_{29}$

4.3 Determination of geothermal water cost

Exergoeconomic cost of geothermal waste water in this paper can be worked out according to the production cost of geothermal water based on the principle of equal exergoeconomic cost of the two-exergy flows in the inlet and outlet[13], that is,

$$\dot{C}_{water}=o*C_{water} \tag{11}$$

Wherein, exergoeconomic cost of geothermal waste water Cwater is worked out according to the following Formula (12), and the values of all contents are shown in Table 3.

Table 3: Fees of the geothermal power plant ($/kW) [21]

Item	C_{exp}	C_{per}	C_d
Value	100~250	10~15	500~1000

Wherein, Cexp denotes survey fee, Cper is license fee, and Cd is drilling fee.

$$C_{water}=(C_{\exp}+C_{per}+C_d)*W_{design} \tag{12}$$

Therefore, the following formula is obtained.

$$C_{water} = C_{22} = \frac{\dot{C}}{\dot{E}} = \frac{(610 \sim 1265) * o * W_{design}}{\dot{m} * e_{22}} \quad (13)$$

Wherein, Wdesign represents designed generated power capacity of the geothermal power plant , kW.

4.4 System evaluation analysis indicators

From the exergoeconomic, exergy and energy points, for each component of the system operating at steady state condition, entering or exiting exergy and energy streams is in the form of heat and work interaction as well as material stream. The associated performance indicators of TSARS in both series and parallel modes used in this paper are expressed in the following equations. Further details see References [26] and [27].

Coefficient of performance (COP) of the system:

$$COP = \frac{Q_{\text{gain}}}{Q_{pay}} \quad (14)$$

Exergy efficiency of the system:

$$\eta_{ex} = \frac{E_{\text{gain}}}{E_{pay}} \quad (15)$$

Exergy loss rate of each component:

$$\xi_i = \frac{\dot{C}_{L,i} + \dot{C}_{D,i}}{\dot{C}_{l,total} + \dot{C}_{D,total}} \quad (16)$$

Exergoeconomic coefficient of each component:

$$f = \frac{Z_i}{Z_i + \dot{C}_{L,i} + \dot{C}_{D,i}} \quad (17)$$

Unit product exergoeconomic cost of chilled water:

$$C_p = \frac{\dot{C}_P}{\dot{E}_P} = \frac{\dot{C}_{28} - \dot{C}_{29}}{\dot{E}_{28} - \dot{E}_{29}} \quad (18)$$

5. RESULTS AND DISCUSSION

5.1 Influence of geothermal water inlet temperature on system thermodynamic performance

Field survey shows that the geothermal waste water discharge temperature in the flash power plant falls in-between 68 ℃ and 75 ℃, due to the influence of power plant operating parameters and environment temperature changes. Figure 5 shows the influence of geothermal water inlet temperature on system thermodynamic performance. On the one hand, when the cooling water inlet temperature of TSARS is up to 28 ℃, and the chilled water outlet temperature of TSARS is 10 ℃. It can be seen in Figure 5a that the COP of both TSARS is continuously improved with the rising of the geothermal water temperature. The maximum COP of parallel TSARS is achieved at 75 ℃, about 0.417. While, COP of series TSARS is also achieved at 75 ℃, about 0.407. This indicates the same relationship between the higher exergy efficiency of the driven heat source and the higher COP of the absorption refrigeration cycles in two-stage, single-effect and multiple-effect absorption refrigeration cycles. On the other hand, it can be seen in Figure 6, that exergy efficiencies of both TSARS are declining with the temperature rising of the geothermal water. For example, exergy efficiency of parallel TSARS at a geothermal water inlet temperature of 70 ℃ is about 14.13%, while exergy efficiency of parallel TSARS at a geothermal water inlet temperature of 74 ℃decreases to13.54%. It reveals an opposite change between COP and exergy efficiency, which lives up to the nature of energy and exergy. Meanwhile, it can be seen in Figures 5a and 5b, that the COP and exergy efficiency of the series TSARS are always larger than that of the parallel TASRS. For example, when the cooling water inlet temperature of TSARS is 28 ℃, the chilled water outlet temperature of TSARS is 10 ℃ and geothermal water inlet temperature of TSARS is 71 ℃. COP and exergy efficiency in the parallel mode TSARS are 0.395 and 14.01% respectively, and they are smaller than 0.400 and 14.23% in series mode TSARS, correspondingly.

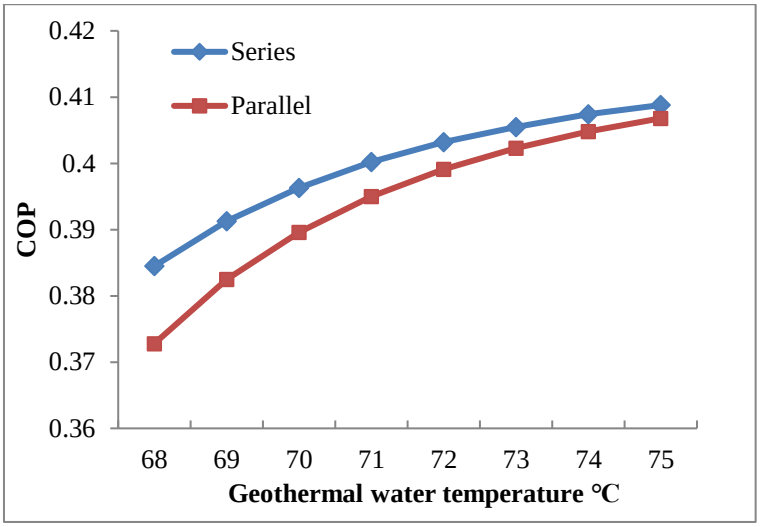

Figure 5: Effects of the waste geothermal water's temperature on COP of TSARS（T29=10℃, T24=28℃, c22=0.211$/GJ）

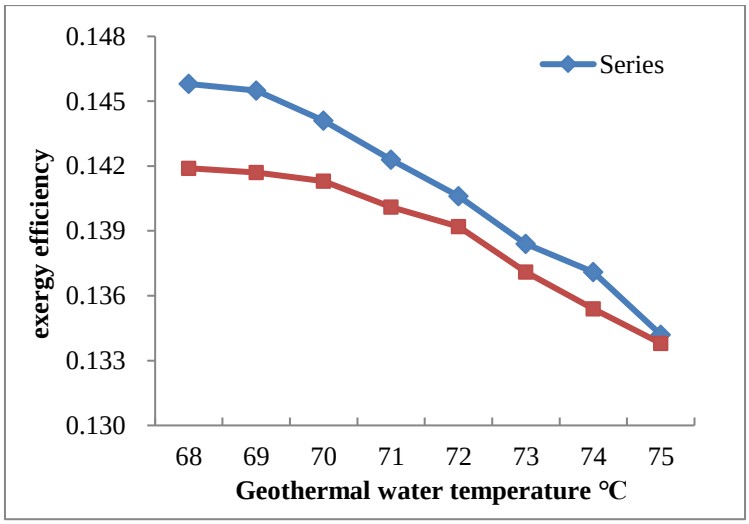

Figure 6: Effects of the waste geothermal water' s temperature on exergy efficiency of TSARS

（T29=10℃, T24=28℃, c22=0.211$/GJ）

5.2 Performance analysis of series and parallel systems

Figure 7 shows effects of the waste geothermal waters cost on the product exergoeconomic cost of the series and parallel TSARS at the cooling water inlet temperature of 28 ℃, the chilled water outlet temperature of 10 ℃ and geothermal water inlet temperature of 71 ℃. It can be seen that, when the geothermal water exergoeconomic cost is 0.21 $/GJ, the unit product exergoeconomic cost of chilled water of TASRS is about 7.73 $ / GJ, while the total input exergy of TSARS is 31.41 kW, the chilled water output exergy is 4.40 kW, and the total exergy loss is 27.01 kW.

On one hand, according to thermodynamics merely, although COP and exergy efficiency are not affected by geothermal water exergoeconomic cost, the parallel TSARS has a lower unit chilled water exergoeconomic cost compared with series TSARS if the cycle thermodynamic and economic performances are considered synchronously. On the other hand, the unit chilled water exergy cost difference increases with the decrease of the geothermal water cost in parallel TSARS and series TSARS. For example, when the geothermal water cost is about 0.14$/GJ, the chilled water exergoeconomic cost of the series mode is about 1.06 times that of the parallel one; when the geothermal water cost is about 0.25$/GJ, the chilled water exergoeconomic cost of the series mode is about 1.04 times that of the parallel one. Furthermore, the geothermal waste water after power generation is cascaded to the parallel TSARS is better than that of series TSARS in the view of exergoeconomic performance, it is opposite only in the thermodynamic performances, such as COP and exergy efficiency.

5.3 Exergoeconomic performance of each subsystem of parallel TSARS

As mentioned above, parallel TSARS is better than series TSARS when both energy and economic performances are concerned. To further analyze the exergoeconomic performance of parallel TSARS, Figures 8 and 9 reveal each equipment exergy loss rate and exergoeconomic coefficient of the parallel TSARS. It is obvious from Figure 8, that the low- and high-pressure generators

contribute a higher heat exchange exergy loss rate due to the greater heat exchange temperature difference, and their exergy loss rate is up to 25.354% and 20.823% respectively, which is followed by condenser and evaporator. It is noted that, total exergy loss of these six heat exchangers accounts for 95% of the total exergy loss of parallel TSARS.

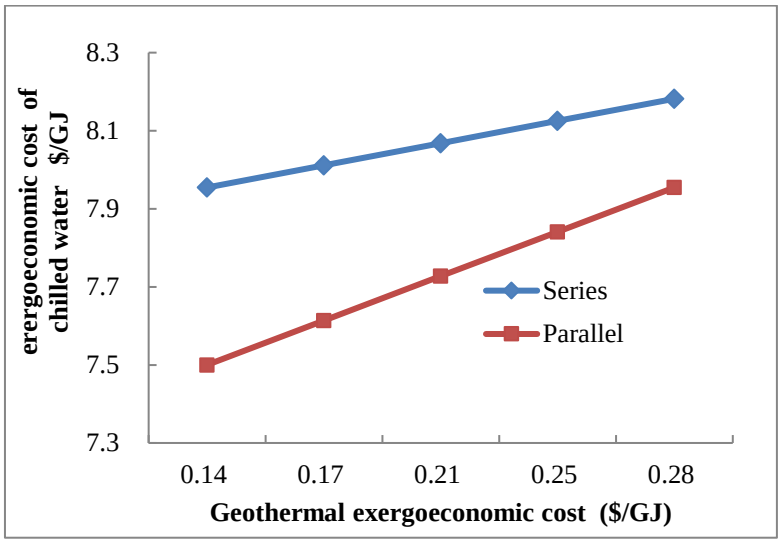

Figure 7: Effects of the waste geothermal waters cost on the product exergoeconomic cost of the series and parallel TSARS （T29=10℃, T24=28℃, T22=71℃）

On the one hand, it can be seen from Figure 9, that exergoeconomic coefficients of the refrigerant throttle valve, condenser as well as high pressure absorber are relatively low, 42.6%, 47.0%, and 51.4% respectively. Because the irreversible loss of these equipments is higher than the equipment investment, the equipment performance can be further improved by increasing the investment and reducing the irreversible loss.

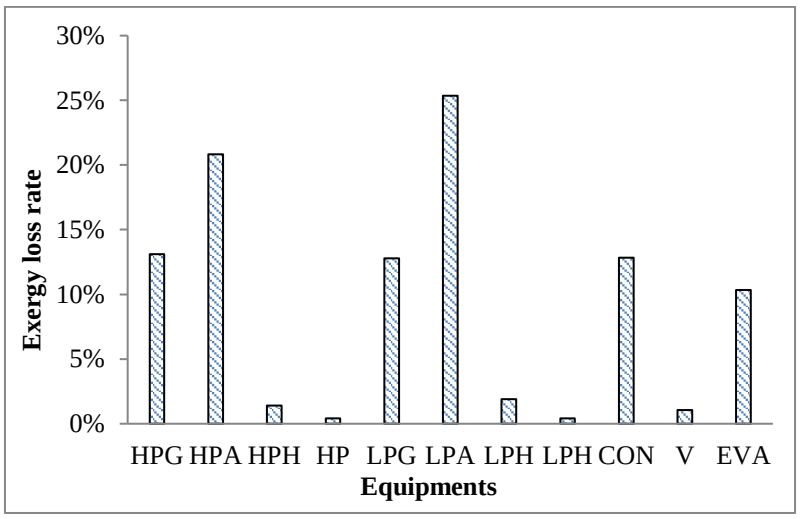

Figure 8: The ξ of each equipment of the parallel TSARS（T22=71℃, T29=10℃, T24=28℃, c22=0.211$/GJ）

6. CONCLUSIONS

It is proposed in the paper that TSARS is cascaded to the existing flash geothermal power plant, to form a cascading comprehensive utilization system of geothermal energy. The cost of geothermal water is determined according to actual operation in the power plant. Then, Exergoeconomics method is adopted for analyzing the modes (series and parallel) of cascading geothermal waste water to TSARS. The following conclusions are drawn:

1) The parallel mode of geothermal water to TSARS has better exergoeconomic performance compared with the series one. The chilled water exergoeconomic cost of Parallel mode is lower than that of the series one;

2) COP and exergy efficiency of series TSARS are always higher than that of the parallel one within the set parameter scope in the paper. COP increases with geothermal water temperature, while the exergy efficiency decreases;

3) The total exergy loss rate of heat exchangers in parallel TSARS is up to 95%, wherein the low pressure absorber has the maximum exergy loss rate because of its maximum irreversible heat transfer temperature difference; refrigerant throttle valve, condenser and high pressure absorber have relatively low exergoeconomic coefficients, which can be improved by increasing the investment or reducing the irreversible loss.

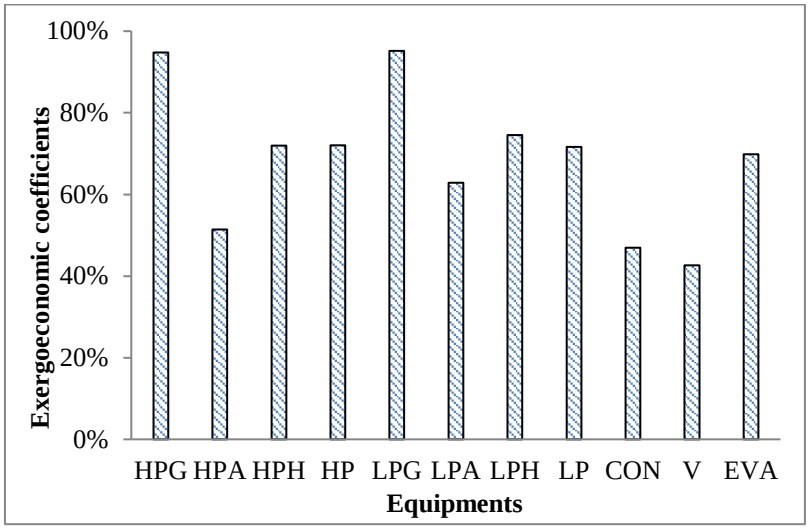

Figure 9:The f of each equipment of the parallel TSARS（T22=71℃, T29=10℃, T24=28℃, c22=0.211$/GJ）

REFERENCES

KamilKaygusuz, AbdullahKaygusuz. Geothermal Energy: Power for a Sustainable Future,Energy Sources, 24, (2002),937-947.

Mahmoudi H, Spahis N, Goosen M F, et al. Application of geothermal energy for heating and fresh water production in a brackish water greenhouse desalination unit: A case study from Algeria,Renewable & Sustainable Energy Reviews, 14(1),(2010),512-517.

Bertani, Ruggero. Geothermal power generation in the world 2010–2014 update report, Geothermics, 60,(2016),31-43.

John W. Lund, Derek H. Freeston,Tonya L. Boyd. Direct utilization of geothermal energy 2010 worldwide review,Geothermics ,2011,40(03):159—180.

Xianglong Luo, Yongzhen Wang, Jun Zhao et. al. Grey relational analysis of an integrated cascade utilization system of geothermal water,International Journal of Green Energy, 13(1), (2016), 14-27

Erdeweghe S V, Bael J V, Laenen B, et al. Feasibility study of a low-temperature geothermal power plant for multiple economic scenarios,Energy, 155, (2018),1004-1012.

Ghaebi H, Farhang B, Parikhani T, et al. Energy, exergy and exergoeconomic analysis of a cogeneration system for power and hydrogen production purpose based on TRR method and using low grade geothermal source,Geothermics, 71, (2018),132-145.

Arslan,O., Kose, R.. Exergoeconomic optimization of integrated geothermal system in Simav, Kutahya,Energy Conversion and Management, 51 (4), (2010), 663—676.

Ratlamwala T A H, Dincer I. Development of a geothermal based integrated system for building multigenerational needs,Energy & Buildings, 2013, 62(62):496-506.

Islam S, Dincer I. Development, analysis and performance assessment of a combined solar and geothermal energy-based integrated system for multigeneration,Solar Energy, 147,(2017),328-343.

Alzaharani A A, Dincer I, Naterer G F. Performance evaluation of a geothermal based integrated system for power, hydrogen and heat generation,International Journal of Hydrogen Energy, 38(34), 2013,14505-14511.

Yuksel Y E, Ozturk M, Dincer I. Energetic and exergetic performance evaluations of a geothermal power plant based integrated system for hydrogen production,International Journal of Hydrogen Energy, 43(1), (2018),78-90.

Salehi S, Mahmoudi S M S, Yari M, et al. Multi-objective optimization of two double-flash geothermal power plants integrated with absorption heat transformation and water desalination,Journal of Cleaner Production, 195, (2018),796-809.

T.A.H. Ratlamwala.I, Dincer, M.A. Gadalla. Performance analysis of a novel integrated geothermal-based system for multi-generation applications,Applied Thermal Engineering, 40(04), (2012),71—79.

Oguz Arslan, Ramazan Kose. Exergoeconomic optimization of integrated geothermal system in Simav, Kutahya,Energy Conversion and Management, 51(04), (2010), 663—676.

Duccio Tempesti. Thermodynamic analysis of two micro CHP systems operating with geothermal and solar energy, Applied Energy, 48(02), (2012),1—9.

Can Coskun, Zuhal Oktay, Ibrahim Dincer. Thermodynamic analyses and case studies of geothermal based multi-generation systems,Energy, 32(06), (2012), 71—80.

Mehmet Kanog lu, Yunus A. C, engel. Economic evaluation of geothermal power generation,heating, and cooling,Energy, 24(06), (1999), 501—509.

W.B Ma, S.M Deng. Theoretical analysis of low-temperature hot source driven two-stage LiBr/H_2O absorption refrigeration system,International Journal of Refrigeration, (1996), 19, 141-146.

A. Sencan, K.A. Yakut, S.A. Kalogirou, Exergy analysis of lithium bromide/water absorption systems,Renewable Energy, 30 (5), (2005), 645—657.

R.D. Misra, P.K. Sahoo, A. Gupta, Thermoeconomic evaluation and optimization of a double-effect H_2O/LiBr vapour-absorption refrigeration system,International Journal of Refrigeration, (2005), 28(3), 331—343.

R.D. Misra, P.K. Sahoo, A. Gupta, Thermoeconomic evaluation and optimization of an aqua-ammonia vapour-absorption refrigeration system,International Journal of Refrigeration, (2006), 29 (1), 47—59.

Lozano MA, Valero A. Theory of the exergetic cost ,Energy, (1993), 18(9), 939-960.

Tsatsaronis G, Javier P. Exergoeconomics evaluation and optimization of energy systems—application to the CGAM problem ,Energy, (1994), 19(3), 287—321.

Bejan A, Tsatsaronis G, Moran M. Thermal design and optimization, New York: John Wiley and Sons Inc; 1996.

Farshi L G, Mahmoudi S M S, Rosen M A. Exergoeconomic comparison of double effect and combined ejector-double effect absorption refrigeration systems ,Applied Energy, (2013), 103(6), 700-711.

Jing Y, Li Z, Liu L, et al. Exergoeconomic Assessment of Solar Absorption and Absorption-Compression Hybrid Refrigeration in Building Cooling ,Entropy, (2018), 20(2), 130-138.